Available online at www.sciencedirect.com
SCIENCE DIRECT®
PERGAMON
International Journal of Heat and Mass Transfer 46 (2003) 2685–2693
International Journal of HEAT and MASS TRANSFER
www.elsevier.com/locate/ijhmt

Choked flow and heat transfer of low density gas in a narrow parallel-plate channel with uniformly heating walls

M. Miyamoto *, W. Shi, Y. Katoh, J. Kurima

Department of Mechanical Engineering, Yamaguchi University, 2-16-1 Tokiwadai, Ube, 755-8611, Japan

Received 20 March 2002; received in revised form 9 October 2002

Abstract

The discharge and heat transfer characteristics of the continuum and slip choked gas flows through a narrow parallel-plate channel with uniform heat flux walls are studied by experimental means, numerical simulation, and analytical approximate solution. The numerical results of the discharge coefficient and the wall surface temperature distributions agree relatively well with the experimental results. The effects of the heat transfer at the walls on the discharge coefficient can be correlated with the dimensionless heat input at the walls. Three kinds of Nusselt numbers which are defined by adiabatic wall, bulk mean, and total temperatures as a reference temperature, respectively, are proposed and the effects of the viscous heating on these Nusselt numbers are clarified.

1. Introduction

The study of the flow and heat transfer of rarefied gas in a narrow channel has become one of the important research topics in various kinds of practical applications such as aerospace engineering, vacuum systems and MEMS. The authors conducted the experiments and 1-D approximate analysis for the choked flows in the channels and nozzles [1], mainly focusing on leakage problems in the vacuum systems. Furthermore, they clarified the characteristics of the choked flow through the parallel-plate channel with adiabatic walls from continuum to slip flow region, through experiments and 2-D numerical analysis [2].

Regarding the study on the microchannel aiming at a micron size channel, there are many publications on the investigations about low-speed isothermal flows, but relatively few publications concerning heat transfer problems. Choi et al. [3], and Wu and Little [4] have measured the overall heat transfer coefficients to a microchannel. And Choi et al. [3] have observed that their obtained Nusselt numbers for the microchannel deviated from the previous correlation for usual macrochannels. Sparrow and Lin [5], and Inmam [6] analytically obtained the Nusselt numbers to incompressible fully developed laminar slip flows in circular tube and in parallel-plate channel, respectively.

But these theoretical studies by Sparrow et al., and Inmam did not take viscous dissipation effects into account. In cases of high-speed internal flows, such as choked flows, when the viscous heating effects cannot be neglected, there seem to be many unsolved primary problems on the heat transfer. For example, when the channel walls are heated or cooled, how does the mass flow rate through the channel vary with the heat transfer? How could the heat transfer coefficient for these cases be defined and estimated? How could this heat transfer coefficient be related to the previous correlations commonly used for low-speed internal flows?

In the present study, in order to answer these primary questions, experiments (for only the heated wall) and two-dimensional numerical analysis, as well as the approximate analytical solution for the choked low-density gas flows (from the continuum to the slip flow region) through a parallel plate channel with the walls heated or cooled by uniform heat flux, were conducted.

* Corresponding author. Tel.: +81-836-85-9106; fax: +81-836-85-9101.
E-mail address: miyamoto@yamaguchi-u.ac.jp (M. Miyamoto).

0017-9310/03/$ - see front matter © 2003 Elsevier Science Ltd. All rights reserved.
doi:10.1016/S0017-9310(03)00030-9

Nomenclature

Br	$\mu u_m^2/(q_w 2h)$ Brinkman number
Cd	discharge coefficient
C_p	specific heat
h	channel height, see Fig. 1
hc	heat transfer coefficient
k	thermal conductivity
Kn	λ/h or $(0.5\pi\gamma)^{0.5}Ma/Re$ Knudsen number
l	channel length
m	mass flow rate
Ma	Mach number
Nu	local Nusselt number
p	pressure
Pr	$C_p\mu/k$ Prandtl number
q	heat flux
Q	$q_w l/[C_p p_{00} h(T_{00}/R)^{0.5}]$ non-dimensional heat input
r	correlation coefficient
R	gas constant
Re	$\rho u_m 2h/\mu$ Reynolds number
T	temperature
u	x-component of velocity
U	maximum velocity at the center of the channel
x, y	spatial coordinates, see Fig. 1

Greek symbols

α	energy accommodation coefficient ($=0.97$)
$\Delta\theta_w$	relative difference between experimental and theoretical results of the dimensionless temperature
γ	ratio of specific heats
δ	$h/2$ half of the channel height
η	y/δ dimensionless form of y
θ	T/T_{00} non-dimensional temperature
λ	molecular mean free path
μ	viscosity
ρ	density
σ	tangential momentum accommodation coefficient ($=1$)

Subscripts

0	channel entrance
00	upstream tank (stagnation state)
aw	adiabatic wall
b	bulk temperature
e	channel exit
e0	downstream tank
R	Rayleigh flow
s	slip flow
T	total temperature
w	channel wall surface
m	average across channel

Superscript

$'$	temperature for adiabatic wall case with the same upstream tank conditions as those for heated wall case

2. Experimental apparatus and method

The experimental devices of this study are generally the same as the former [2]. Fig. 1 schematically shows the geometry of the parallel-plate channel and the thermocouple positions. The left end of the channel block is fastened to the flange by screws, which is installed in a 300 mm-diameter vacuum tank to separate it into two parts. The left part is named the upstream tank while the right part, the downstream tank.

After mass flow rate is measured by laminar type flow meters, dry clean air flows into the upstream tank, then passes through the channel, and finally is exhausted from the downstream tank into vacuum pumps.

With the aim of reducing the convection heat loss from the channel outer surfaces, the whole channel block is exposed to the lower pressure of the downstream tank. In addition, in order to decrease the heat conduction through the channel block to the flange, two circular grooves are slotted in the inlet side of the channel block to which the flange attaches, as shown in Fig. 1.

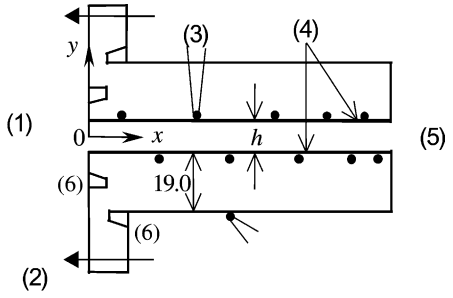

(1): upstream tank. (2): Screw to flange.
(3): thermocouple. (4): Nickel-plated surfaces.
(5): downstream tank. (6):Circular groove

Fig. 1. Parallel-plate channel.

The parallel-plate channel is 1.0 mm high, 120 mm in length, and 50.5 mm in width. It is made of phenolic resin. The inner surfaces of the channel are plated with nickel of 1 μm thickness. DC is supplied to the two sides of the plated layers to generate a uniform surface heat flux. The wall surface temperature distribution is measured by 10 thermocouples (Type E with the diameter of 25 μm) which are embedded behind the plated layer.

In all the experiments for $0.29 < p_{00} < 25.2$ kPa ($2.2 < p_{00} < 189$ Torr) and $106 < q_w < 3058$ W/m^2, to obtain a choked flow state, the pressure ratios of p_{e0}/p_{00} were kept under about 1/10. The upstream tank temperatures were always kept at room temperature (≒300 K).

3. Numerical procedure

The present numerical procedure is almost the same as the previous study [2]. The isentropic flow is assumed from the upstream tank to the channel inlet. The velocity and temperature fields in the channel are calculated by the following governing equations, based on the boundary layer approximation, and the boundary conditions, in which the velocity slip, temperature jump, and slip work on the walls are taken into account. Here, x axis is set on the channel center line along the streamwise direction, and $x = 0$ at the channel inlet. y axis is perpendicular to the x axis and the walls locate at $y = \pm h/2$.

$$\frac{\partial}{\partial x}(\rho u) + \frac{\partial}{\partial y}(\rho v) = 0 \tag{1}$$

$$\rho\left(u\frac{\partial u}{\partial x} + v\frac{\partial u}{\partial y}\right) = -\frac{\mathrm{d}p}{\mathrm{d}x} + \frac{\partial}{\partial y}\left(\mu\frac{\partial u}{\partial y}\right) \tag{2}$$

$$\rho c_p\left(u\frac{\partial T}{\partial x} + v\frac{\partial T}{\partial y}\right) = u\frac{\mathrm{d}p}{\mathrm{d}x} + \frac{\partial}{\partial y}\left(k\frac{\partial T}{\partial y}\right) + \mu\left(\frac{\partial u}{\partial y}\right)^2 \tag{3}$$

$$p = \rho RT \tag{4}$$

The boundary conditions only at the wall of $y = -h/2$ are given here as follows [5]:

The slip velocity u_s at the wall:

$$u_{y=-h/2} \equiv u_s = \frac{2-\sigma}{\sigma}\lambda\left(\frac{\partial u}{\partial y}\right)_{y=-h/2} + \frac{3}{4}\frac{\mu}{\rho T}\left(\frac{\partial T}{\partial x}\right)_{y=-h/2} \tag{5}$$

The temperature jump at the wall:

$$T_w = T_{y=-h/2} - \frac{2-\alpha}{\alpha}\frac{2\gamma}{\gamma+1}\frac{\lambda}{Pr}\left(\frac{\partial T}{\partial y}\right)_{y=-h/2} + \frac{1}{c_p}\frac{4\gamma}{\gamma+1}\frac{1-\alpha}{\alpha}\frac{\sigma}{2-\sigma}u_s^2 \tag{6}$$

The energy equilibrium at the wall:

$$k\left(\frac{\partial T}{\partial y}\right)_{y=-h/2} = -q_w - \mu u_s\left(\frac{\partial u}{\partial y}\right)_{y=-h/2} \tag{7}$$

The basic equations are numerically solved by the finite difference method using the forward marching scheme from the channel inlet in a similar manner to Kashiwagi et al. [7]. The temperature dependence of viscosity and thermal conductivity is evaluated also by the same equations as Kashiwagi. But the present numerical method [2] is improved to accomplish higher precision for choked flow state in the lower pressure region (in the upstream tank) than Kashiwagi's method.

4. Comparison of experimental and numerical results and discussion

4.1. Discharge coefficient

The flow from the upstream tank to the channel inlet can be assumed to be isentropic so that there exists the following relationship between the mass flow rate m and the inlet Mach number Ma_0.

$$\frac{m}{m_0} = Ma_0\left[\frac{\gamma+1}{2+(\gamma-1)Ma_0^2}\right]^{\frac{\gamma+1}{2(\gamma-1)}}, \tag{8}$$

where m_0 is the maximum flow rate of the choked isentropic flow ($Ma_0 = 1$). On the other hand, the inviscid compressible flow through the parallel channel with heat transfer walls is well known as Rayleigh flow. When the Rayleigh flow is choked, i.e. the channel exit Mach number reaches 1, the relationship between the wall heat flux and the mass flow rate can be expressed as [8]:

$$\frac{(Ma_0^2-1)^2}{(\gamma+1)Ma_0^2[2+(\gamma-1)Ma_0^2]} = \frac{2q_w l}{m_R C_p T_{00}}, \tag{9}$$

where m_R is the mass flow rate of the choked Rayleigh flow. Combining Eqs. (8) and (9) and letting $m = m_R$, the mass flow rate of the choked Rayleigh flow can be numerically calculated.

Fig. 2 shows the comparison of the discharge coefficients plotted against the dimensionless heat input, Q that is deduced from the Rayleigh flow solution, Eq. (9). Where Cd_R is the discharge coefficient of the choked Rayleigh flow. And Cd_{aw} and Cd_{hw} means the present numerical and experimental results for the cases when the walls are adiabatic and heated, respectively. All these discharge coefficients are defined as the ratio of the mass flow rates to that of the choked isentropic flow with the same upstream tank conditions. Cd_{hw} includes the viscous effects so that Cd_{hw}/Cd_{aw} is employed as the ordinate to eliminate the viscous effects. The plotted values of Cd_{hw}/Cd_{aw} obtained from the present numerical solutions seem to be well correlated with Q, as shown in Fig. 2 and can be approximated by Eq. (10b) for $0 < Q < 0.2$. The slight scatter of the numerical results in Fig. 2 can be considered to be mainly attributed to the

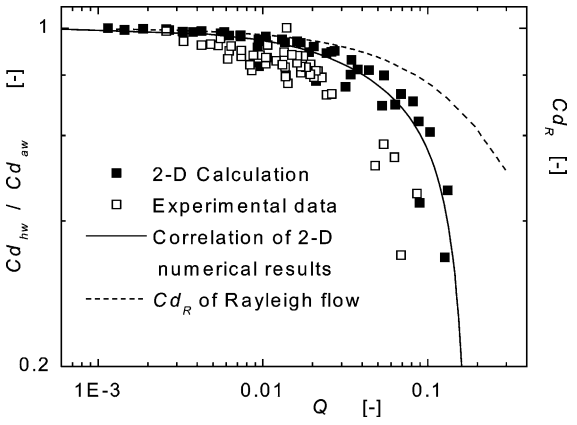

Fig. 2. Comparison of discharge coefficients.

temperature dependence of the viscosity, because the plotted points with the same Q ($\approx q_w/p_{00}$) have different gas temperature distributions along the channel. In the numerical solutions, the viscosity of the gas is proportional to $(T/T_{00})^{0.76}$ [2]. When p_{00} becomes small, the temperature of the gas becomes very high due to the reduction of the mass flow rate, even if Q is constant. The effects of the temperature dependence of the viscosity can not be eliminated even by using the ratio Cd_{hw}/Cd_{aw}.

The experimental data show a little lower than the numerical results. When the dimensionless heat input becomes large, the Rayleigh flow gives a higher discharge coefficient, Cd_R (which is indicated by a dashed line and can be approximated by Eq. (10a)), than the present numerical and experimental results, because the effects of the heating on the mass flow rate relatively increase due to the reduced mass flow rate caused by the viscosity.

$$Cd_R = 1.0 - 2.93Q + 7.12Q^2 - 9.50Q^3 \quad (|r| = 1.00) \tag{10a}$$

$$Cd_{hw}/Cd_{aw} = 1.0 - 5.85Q + 29.4Q^2 - 149.0Q^3 \quad (|r| = 0.95) \tag{10b}$$

It is shown in the figure that the normalized distribution of discharge coefficients obtained from the numerical solution is abruptly reduced when the dimensionless heat input Q becomes larger than about 0.1. This fact seems to be very important for practical applications like the leakage problems.

4.2. Distributions of wall surface temperature

The dimensionless wall surface temperature distributions of the experimental and numerical results are compared in Fig. 3. The experimental results agree rel-

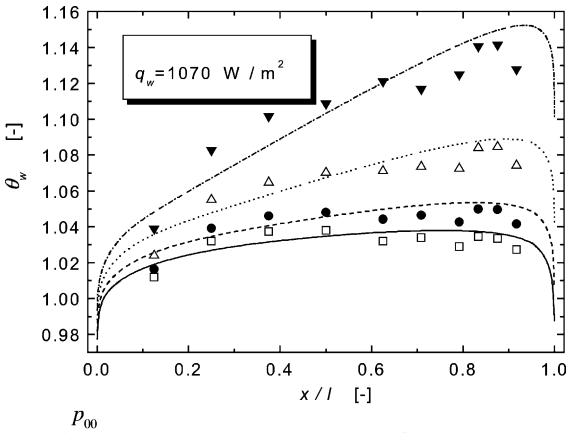

	p_{00} kPa	Ma_0	Kn_0	Re_0	Br_0	Cal.	Exp.	$\Delta\theta_w$
(4):	6.7,	0.21,	1.0×10^{-3},	624,	0.043	----------	▼	2.1%
(3):	9.3,	0.26,	7.4×10^{-4},	1068,	0.066	.....	△	1.3%
(2):	13.3,	0.31,	5.2×10^{-4},	1803,	0.094	--------	●	1.0%
(1):	17.3,	0.35,	4.1×10^{-4},	2578,	0.116	———	□	0.8%

Fig. 3. Wall surface temperature profiles along channel.

atively well with the theoretical distributions. When the pressure p_{00} is lower, the flow becomes fully developed in a shorter distance from the inlet due to the decrease of the mass flow rate and Reynolds number. Consequently the wall temperature distributions become high and linear in almost the entire channel. When the pressure p_{00} is lower than about 4 kPa (= 30 Torr, not shown in the figure), the differences between the theoretical and experimental results become large. One of the main reasons of these relatively large differences can be considered to result from the heat conduction in the walls of the experiment. The heat conduction in the walls makes the wall surface temperature distribution more uniform. The experimental results in Fig. 3 also show a slight tendency in this regard. In the experiment, the lower the pressure, p_{00} becomes, the more difficult it is to maintain the uniform convective heat flux condition on the walls, because the heat conduction in the walls becomes relatively large in comparison to the small convection heat transfer in the channel.

4.3. Distributions of local Nusselt number

McAdams et al. [9] and Kashiwagi et al. [7] proposed the local Nusselt number defined by using the adiabatic wall temperature, as expressed by Eq. (11), for the heat transfer to the high speed internal flow.

$$Nu'_a = \frac{2h}{k}\frac{q_w}{T_w - T'_{aw}} \tag{11}$$

In Fig. 4, the distributions of the local Nusselt number defined by Eq. (11) and calculated from the present

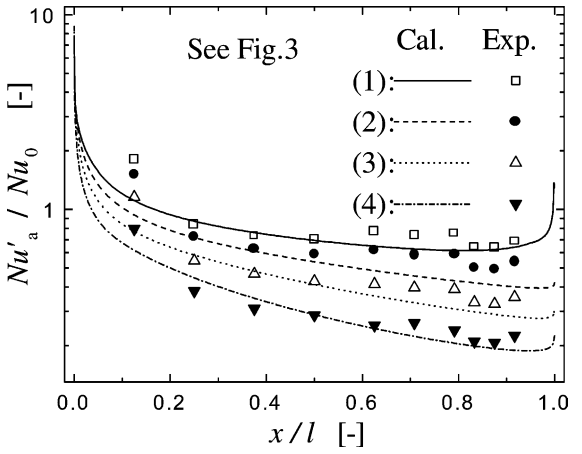

Fig. 4. Comparison of local Nu'_a profiles.

results shown in Fig. 3 are compared. But the reference temperature T'_{aw} in these comparisons is the adiabatic wall temperature at the same location, x and with the same upstream tank conditions as those in the case when the walls are heated. (T'_{aw} must be distinguished from T_{aw} which will be discussed in Section 5.) As shown in Fig. 4, the numerical solutions and the experimental results agree relatively well, but when the pressure is lower than 4 kPa (= 30 Torr, not shown in the figure), the measured local Nusselt numbers become higher than the theoretical values at the down stream location. These deviations caused by the conduction in the walls correspond to those of the wall surface temperature distributions.

The ordinate in Fig. 4 is the Nusselt number, Nu'_a normalized by Nu_0, the well-known Nusselt number of the developed incompressible (i.e. low-speed) laminar internal flow, which is defined by the bulk-mean fluid temperature instead of T'_{aw} and is equal to 140/17. It is important to observe that the Nusselt number defined by T'_{aw} as Eq. (11) does not approach to Nu_0 even at the limit when the velocity becomes slow and the viscous heating can be neglected, as also discussed in Section 5.

5. Analytical solution of fully developed incompressible flow

5.1. Bulk mean fluid temperature and adiabatic wall temperature

Most of the microchannel is very long compared with its cross section, so that the flow through the microchannel can be considered to be fully developed in most of the channel. When the flow is incompressible and fully developed, the analytical solutions of the velocity and temperature can be easily obtained from the governing equations, Eqs. (1)–(3) with the assumption of the constant physical properties. The wall heat flux q_w is constant along the channel. The boundary conditions of the velocity slip and the temperature jump can be simplified by neglecting the higher-order small terms as following; the 2nd term in the right-hand side of Eq. (5) and 3rd term in the right-hand side of Eq. (6) are relatively small compared with the other terms and can be neglected. In this section, the effects of the viscous heating and the rarefaction on the heat transfer at the walls will be examined using the obtained analytical solution.

The solutions obtained by using the above stated conditions are given as follows:

The velocity profile:

$$\frac{u}{U} = \frac{b-\eta^2}{b} \tag{12}$$

The temperature profile:

$$T = T_w - 2Kn\beta\left[\frac{2U^2(b-1)}{C_p b^2} + \frac{\delta q_w}{Prk}\right] + \frac{U^2 Pr}{2C_p b^2}[1-\eta^4-2b(1-\eta^2)] + \frac{\delta q_w}{(3b-1)4k}[1-\eta^4-6b(1-\eta^2)] \tag{13}$$

Here $\eta = y/\delta$ and U is the maximum velocity at the center of the channel. U, b, β, and ξ are given by the following equations:

$$U = -\frac{\delta^2 b}{2\mu}\frac{dp}{dx} \quad b = 1 + 4\frac{2-\sigma}{\sigma}Kn$$
$$\beta = \frac{2-\alpha}{\alpha}\frac{2\gamma}{\gamma+1} \quad \xi = \frac{2-\sigma}{\sigma} \tag{14}$$

In the right-hand side of Eq. (13), the second term is the temperature jump at the wall, the third term is the viscous heating term, and the fourth term indicates the heating by the wall heat flux. The velocity field of the obtained solution is basically independent of the temperature field because of the assumption of the constant physical properties, and is a function of the given pressure gradient along the channel.

The bulk mean fluid temperature, T_b calculated from the obtained profiles of the velocity and the temperature is written as:

$$T_w - T_b = \frac{\delta q_w}{k}\left[\frac{17+168\xi Kn+420(\xi Kn)^2}{35(1+6\xi Kn)^2} + \frac{2\beta Kn}{Pr}\right] + \frac{4U^2 Pr}{C_p(1+4\xi Kn)^2}\left[\frac{3+42\xi Kn+140(\xi Kn)^2}{35(1+6\xi Kn)} + \frac{4\beta\xi Kn^2}{Pr}\right] \tag{15}$$

The second term of the right-hand side of Eq. (15) is the viscous heating term and is always positive. The first term indicates the heating by the wall heat flux.

When q_w becomes 0 in Eq. (15) and thus T_w becomes T'_{aw}, Eq. (15) gives the following Eq. (16).

$$T'_{aw} - T'_b = \frac{4U^2 Pr}{C_p(1+4\xi Kn)^2}\left[\frac{3+42\xi Kn+140(\xi Kn)^2}{35(1+6\xi Kn)}+\frac{4\beta Kn^2}{Pr}\right] \tag{16}$$

Here T'_b is the bulk mean fluid temperature at location x for the case of the adiabatic walls and is different from T_b at the same x for the heated wall case. As a matter of course, the upstream tank conditions for T'_b and T_b are the same. The right-hand side of Eq. (16) is just the viscous heating term.

As shown by Eq. (15), if $T_w - T_b$ is used as the temperature difference to define the heat transfer coefficient, hc, like $q_w = hc(T_w - T_b)$, especially when the viscous heating term becomes large or q_w is small, it is possible that the signs of $T_w - T_b$ and q_w are different from each other due to the existence of the viscous heating term. This means that the negative heat transfer coefficient is possible. If the viscous heating term can be eliminated from the temperature difference, the difficulty raised by the negative heat transfer coefficient can be avoided. Therefore, McAdams et al. [9] and Kashiwagi et al. [7] proposed using the temperature difference, $T_w - T'_{aw}$, as shown in Eq. (11). $T_w - T'_{aw}$ is given by Eq. (17)

$$\begin{aligned} T_w - T'_{aw} &= T_w - T_b - (T'_{aw} - T'_b) + (T_b - T'_b) \\ &= \frac{\delta q_w}{k}\left[\frac{17+168\xi Kn+420(\xi Kn)^2}{35(1+6\xi Kn)^2}+\frac{2\beta Kn}{Pr}\right] \\ &\quad + (T_b - T'_b) \end{aligned} \tag{17}$$

For the case of the uniform wall heat flux, the term $(T_b - T'_b)$ is equal to $2q_w x/(C_p m)$ by conservation of energy. Here, $2q_w x$ is the heat transferred from the walls between the entrance and x. But this assumes that the difference of kinetic energy between the flows corresponding to T_b and T'_b can be neglected. The heat transfer coefficient defined by the temperature difference, $T_w - T'_{aw}$, does not seem to become negative. The viscous heating term can apparently be eliminated from the temperature difference, $T_w - T'_{aw}$, but even when the flow velocity becomes so low that the viscous heating term can be neglected, $T_w - T'_{aw}$ does not become equal to $T_w - T_b$, because the temperature difference $T_b - T'_b$ remains as shown by Eq. (17). In the following, the three kinds of Nusselt numbers defined by the different temperature differences will be proposed.

5.2. Nusselt numbers based on three kinds of reference temperatures

In the definition of the heat transfer coefficient for the high-speed uniform external flow with viscous dissipation, the adiabatic wall temperature is usually used as a reference temperature instead of the uniform stream temperature for the low-speed external flow. It is because the heat transfer rate to the high-speed flow can be calculated with the same correlation used for the low-speed flow without viscous dissipation only by this substitution of the reference temperature [10]. In the case of the internal flow, the situation is not so simple as that in the external flow as shown before in 5.1.

In the first place, the following modified adiabatic wall temperature T_{aw} is proposed:

$$T_{aw} = T'_{aw} + (T_b - T'_b) \tag{18}$$

(If Eq. (18) is rewritten like $T_{aw} = T_b + (T'_{aw} - T'_b)$, T_{aw} can be also considered to be the modified form of the bulk temperature, T_b.)

As mentioned before, $(T_b - T'_b)$ is closely related to the heat transfer on the walls and can be evaluated by $T_b - T'_b = 2q_w x/(C_p m)$ for the uniform wall heat flux. Now, the difference between T'_{aw} and T_{aw} used as a reference temperature to define the heat transfer coefficient is explained as follows: T'_{aw} is the temperature at the location, x, on the adiabatic wall for the flow with the same upstream tank conditions as that of the corresponding heated wall case. It should be noted that the stagnation (or total) temperature is constant along the channel with the adiabatic walls. On the other hand, T_{aw} is also the temperature at the location, x, on the adiabatic wall except for the flow with the same stagnation temperature as the stagnation temperature at the x for the heated wall case, which is different from the temperature at the upstream tank for the heated wall case. T_{aw} is the adiabatic wall temperature for the stagnation condition including the heat transfer effect from the upper stream walls. From Eqs. (17) and (18), the Nusselt number defined by the adiabatic wall temperature, T_{aw}, as a reference temperature is given by Eq. (19).

$$\begin{aligned} Nu_a &= \frac{2h}{k}\frac{q_w}{T_w - T_{aw}} \\ &= \frac{140(1+6\xi Kn)^2 Pr}{[17+168\xi Kn+420(\xi Kn)^2]Pr+70\beta Kn(1+6\xi Kn)^2} \end{aligned} \tag{19}$$

Nu_a given by Eq. (19) is the same as the usual Nusselt number for the low-speed flow without the viscous dissipation, which is defined by the bulk mean fluid temperature as the reference temperature. And at the limit $Kn = 0$, $Nu_a = 140/17 = Nu_0$. Nu_a given by Eq. (19) is different from Nu'_a given by Eq. (11), which was proposed

by McAdams and Kashiwagi. They did not take the stream-wise change of the stagnation (or total) temperature with the heating or cooling into account. Sparrow et al. [5] and Inmam [6] obtained the Nusselt number similar to Eq. (19) for a tube and a parallel channel, respectively, using the bulk mean fluid temperature as a reference temperature.

In the second place, when the bulk mean fluid temperature, T_b is employed as a reference temperature, the following Nusselt number, Eq. (20) is obtained from Eq. (15). In this case, the viscous dissipation term (the first term of right hand side of Eq. (20)) is not eliminated for the high-speed flow. Eq. (20) is expressed in the reciprocal form of the Nusselt number for simplicity.

$$\frac{1}{Nu_b} = \frac{k(T_w - T_b)}{2hq_w} = \frac{9Br}{(1+6\xi Kn)^2}\left[\frac{3+42\xi Kn+140(\xi Kn)^2}{35(1+6\xi Kn)} + \frac{4\beta\xi Kn^2}{Pr}\right] + \frac{17+168\xi Kn+420(\xi Kn)^2}{140(1+6\xi Kn)^2} + \frac{\beta Kn}{2Pr} \quad (20)$$

At the limit case $Kn = 0$, $Nu_b = 140/(17 + 108Br)$. This is the same as the previous Nusselt number [11] defined by the bulk mean temperature for the fully developed incompressible flow with the viscous dissipation.

In the third place, when the bulk mean total temperature, $T_T(= T_b + (u^2)_m/(2C_p))$ is employed as a reference temperature, the following Nusselt number, Eq. (21) is obtained. This can be considered to be equivalent to the Nusselt number measured by Choi et al. [3] who determined the Nusselt number by measurements of the temperatures at the upstream and down stream tanks.

$$\frac{1}{Nu_T} = \frac{k(T_w - T_T)}{2hq_w} = \frac{17+168\xi Kn+420(\xi Kn)^2}{140(1+6\xi Kn)^2} + \frac{\beta Kn}{2Pr} + \frac{9Br}{35Pr(1+6\xi Kn)^3}\Big\{Pr[3+42\xi Kn + 140(\xi Kn)^2] - 3[1+14\xi Kn+70(\xi Kn)^2 + 140(\xi Kn)^3] + 140\beta\xi Kn^2(1+6\xi Kn)^2\Big\} \quad (21)$$

At the limit case $Kn = 0$, $Nu_T = 140/[17 - 108Br(1/Pr - 1)]$.

For the accommodation coefficients of the usual wall surface ($\alpha \fallingdotseq 1$ and $\sigma \fallingdotseq 1$), all these Nusselt numbers (Nu_a, Nu_b and Nu_T given by Eqs. (19)–(21), respectively) decrease with the increase of Kn (see Figs. 5 and 6).

The expressions of the Nusselt numbers, Nu_b and Nu_T, in Eqs. (20) and (21), include the Brinkman number

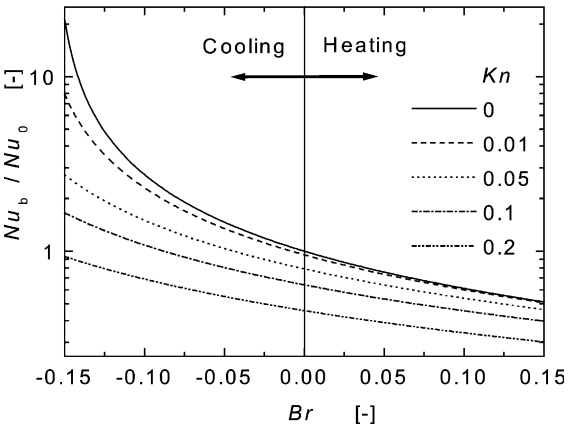

Fig. 5. Relationship of Nu_b–Kn–Br ($Pr = 0.7$, $\alpha = 1$, $\sigma = 1$).

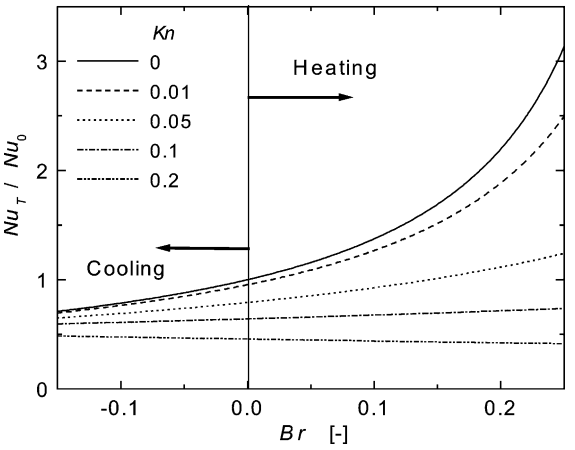

Fig. 6. Relationship of Nu_T–Kn–Br ($Pr = 0.7$, $\alpha = 1$, $\sigma = 1$).

which indicates the effects of the viscous dissipation. Although these equations are conducted for the heating wall condition ($q_w > 0$), these are also applicable to the cooling condition ($q_w < 0$) by changing the sign of the Brinkman number from $+Br$ to $-Br$. Accordingly, the viscous dissipation terms in Eqs. (20) and (21) have the different signs corresponding to the cooling wall and the heating wall. And if the Brinkman number becomes large, the Nusselt number could become infinity, and furthermore become negative. For example, it is possible that Nu_b for cooling and Nu_T for heating become negative. This means that the definition of the Nusselt number must be chosen based on the cooling or heating conditions on the walls.

The Nusselt numbers, Nu_b and Nu_T, are normalized by Nu_0 and are plotted against the Brinkman number, Br, in Figs. 5 and 6, respectively. When $Br = 0$, Nu_b/Nu_0 in Fig. 5 corresponds to Nu_a/Nu_0. Here Nu_a is given by

Eq. (19). These figures clearly indicate the above stated characteristics of the three kinds of Nusselt number.

6. Numerical solutions of local Nusselt numbers based on three kinds of reference temperature

The three kinds of the Nusselt numbers, which have been applied to the incompressible developed flow in Section 5, are evaluated from the present numerical solutions corresponding to the wall surface temperature distributions shown in Fig. 3. These are normalized by Nu_0 for the fully developed low-speed flow and are shown in Fig. 7(a)–(c).

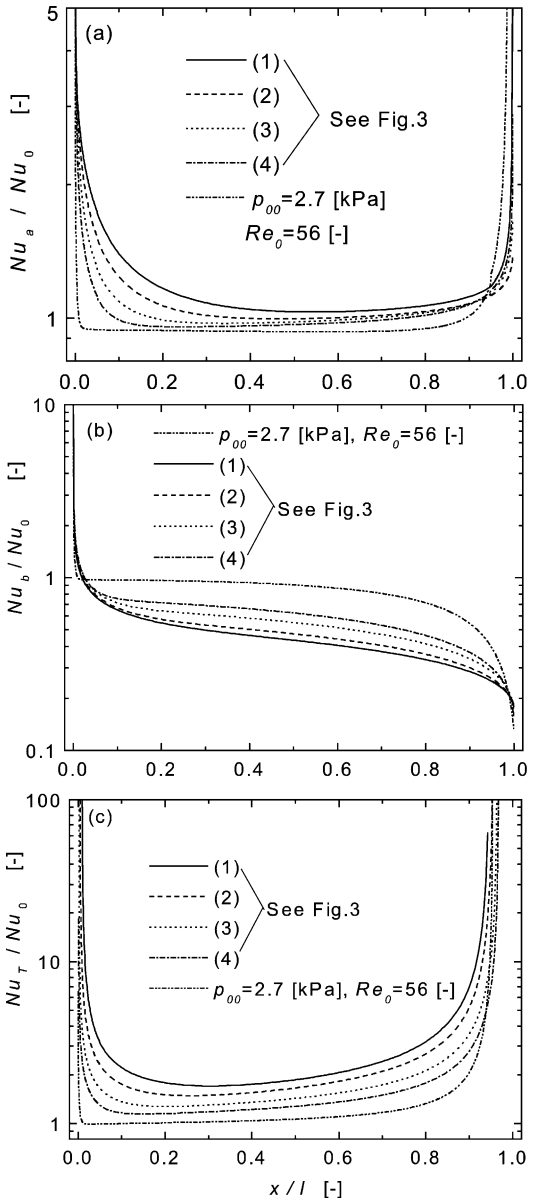

Fig. 7. Numerical results of Nusselt number distributions based on different reference temperature.

The normalized distributions of Nu_a defined by the adiabatic wall temperature, T_{aw} like Eq. (19) are shown in Fig. 7(a). This T_{aw} is approximately evaluated by $T_{aw} = T'_{aw} + 2q_w x/(C_p m)$, neglecting the difference of the kinetic energy between the flows corresponding to T_{aw} and T'_{aw}. If the experimental results were replotted in Fig. 7(a), the relationship between the experimental and theoretical results would be qualitatively the same as that shown in Fig. 4 and the quantitative differences between them would be relatively enlarged in Fig. 7(a) compared to Fig. 4.

As shown in these figures, these Nusselt numbers abruptly change near the inlet and exit, because the entrance developing flow, and the rapid acceleration just before the Mach number reaches 1 around the exit, occur. Nu_T in Fig. 7(c) becomes negative very near $x/l = 1$. The negative values of Nu_T are not shown in Fig. 7(c) because of the logarithmic coordinate axes in the figure. The small blank space between the right side ends of the plotted lines of Nu_T/Nu_0 and $x/l = 1$ in Fig. 7(c) indicates the existence of the negative values of Nu_T.

As the upstream tank pressure decreases, these normalized Nusselt number distributions gradually approach 1 throughout the channel. And when $p_{00} = 2.7$ kPa, the minimum pressure in the figures, the normalized local Nusselt numbers, Nu_a and Nu_b, become locally lower than 1 due to the rarefaction effect, such as velocity slip and temperature jump at the walls.

7. Conclusions

The choked low-density gas flow (from the continuum to the slip flow region) through the parallel plate channel (1 mm in height and 120 mm in length) with the uniform heat flux walls have been studied by experimental means, the finite difference numerical simulation, and the analytical approximate solution. The main concluding remarks are summarized as follows:

(1) The decrease of the mass flow rate by the heated walls is well correlated by using the dimensionless heat input Q at the walls and the ratio of the mass flow rate to that for the case of the adiabatic walls. This ratio of the mass flow rates abruptly decrease when Q becomes greater than 0.1.
(2) The experimental results of the wall surface temperature distributions generally agree well with the numerical solutions, except the cases where $p_{00} < 4$ kPa (30 Torr).
(3) The three kinds of the local Nusselt numbers, Nu_a, Nu_b and Nu_T, defined using the adiabatic wall temperature, the bulk mean fluid temperature, and the

mean total temperature, respectively, are proposed and the analytical expressions of these Nusselt numbers are obtained for the fully developed incompressible flow. The effects of the viscous dissipation and the rarefaction on these Nusselt number are clarified.

(4) As the upstream tank pressure becomes low, the numerically calculated distributions of the three proposed local Nusselt numbers for the heated walls approaches Nu_0 ($=140/17$) throughout the channel, except near the entrance and exit.

Acknowledgements

The authors greatly appreciate the support by Dr. Etsuro Hirai, Hiroshima Research Institute of Mitsubishi Heavy Industry Ltd., in a manufacture of the experimental apparatus, and also the support by Grant-in-Aid for Scientific Research (C) from Japanese Government.

References

[1] T. Taguchi, K. Yanagi, M. Miyamoto, T. Nagata, Precise discharge characteristics of rarefied critical flows through a parallel plate channel, in: J. Harvey, G. Lord (Eds.), Rarefied Gas Dynamics 19, vol. 1, Oxford University Press, 1995, pp. 382–388.

[2] W. Shi, M. Miyamoto, Y. Katoh, J. Kurima, Choked flow of low density gas in a narrow parallel-plate channel with adiabatic walls, Int. J. Heat Mass Transfer 44 (13) (2001) 2555–2565.

[3] S.B. Choi, R.F. Barron, R.O. Warrington, Fluid flow and heat transfer in microtubes, Micromech. Sensor. Actuat. Syst. ASME DSC-32 (1991) 123–134.

[4] P. Wu, W.A. Little, Measurement of the heat transfer characteristics of gas flow in fine channel exchangers used for microminiature refrigerators, Cryogenics 24 (1984) 415–420.

[5] E.M. Sparrow, S.H. Lin, Laminar heat transfer in tubes under slip-flow conditions, J. Heat Transfer Trans. ASME (1962) 363–369.

[6] R.M. Inman, Laminar slip flow heat transfer in a parallel plate channel or a round tube with uniform wall heating, NASA TN D-2393, 1964.

[7] T. Kashiwagi, N. Isshiki, Y. Kurosaki, Heat transfer of the critical air flow in a nozzle (1st Report: Numerical study on heat transfer of the critical air flow in a nozzle with parallel walls), Bull. JSME 22–163 (1979) 63–70.

[8] A.H. Shapiro, The Dynamics and Thermodynamics of Compressible Fluid Flow, vol. I, Ronald Press, New York, 1953 (pp. 73–111).

[9] W.H. McAdams, L.A. Nicolai, J.H. Keenan, Measurement of recovery factors and coefficient of heat transfer in a tube for subsonic flow of air, AIChE 42 (1946) 907–925.

[10] J.P. Holman, Heat Transfer, eighth ed., McGraw-Hill, London, 1997, pp. 254–264.

[11] R.K. Shah, A.L. London, Laminar Flow Forced Convection in Ducts, Supp. 1 of Advances in Heat Transfer, Academic Press, 1978.